PHYSICAL REVIEW A **79**, 051801(R) (2009)

Guiding electromagnetic energy below the diffraction limit with dielectric particle arrays

Junjie Du,[1,2] Shiyang Liu,[1,2] Zhifang Lin,[1] Jian Zi,[1] and S. T. Chui[2]
[1]*Department of Physics, Surface Physics Laboratory, Fudan University, Shanghai 200433, China*
[2]*Bartol Research Institute, University of Delaware, Newark, Delaware 19716, USA*
(Received 25 September 2008; published 27 May 2009)

We demonstrate that electromagnetic energy can be efficiently guided along a single chain, around a corner, and split at forked structures below the diffraction limit with the use of appropriate dielectric particle arrays. The fields are confined to a region with the transverse width less than half of the guided wavelength. Our results give an explicit demonstration that the dielectric based subwavelength photonic circuit is achievable, providing an alternative to the surface-plasmon-based metallic counterpart.

DOI: 10.1103/PhysRevA.79.051801 PACS number(s): 42.79.Gn, 42.82.Et, 73.20.Mf

Miniaturization of photonic elements and efficient transport of electromagnetic (EM) energy are two paramount issues required for the design of integrated photonic circuits. Conventional dielectric waveguides can support nearly lossless light propagation. But they usually suffer from the diffraction limit (DL), which demands that the transverse size of a waveguide must be larger than half the wavelength of the guided wave, making its miniaturization difficult. As a way to circumvent the DL, linear arrays of metallic nanoparticles, termed metallic plasmon waveguides (MPWGs), have been extensively studied and demonstrated to be able to guide light energy at nanoscale with nearly no radiative loss [1–12]. However, the intrinsic material loss in metal is inevitable and severely limits the applications of the surface-plasmon-based metallic waveguides.

In this Rapid Communication, based on rigorous numerical calculations, we examine the response of the subwavelength dielectric waveguide (SDWG) systems to the EM wave under photonic circuit conditions. The efficient transport of EM energy below the DL is manifested through guiding the energy along a straight chain, around a corner, as well as splitting the EM energy at typical bifurcate structures, with nearly no radiative and material loss. Our results indicate that the SDWGs made of dielectric particle arrays can display similar behavior in energy transfer as MPWGs, paving an alternative way toward integrated optics to the surface-plasmon-based metallic counterpart.

Let us start with the basic physics of the waveguide modes in the MPWGs. To transport EM energy without radiative loss, the waveguide modes must have an imaginary transverse wave vector $k_\perp$ normal to the propagating direction. Roughly, $k_\perp$ can be approximated by $k_\perp = \sqrt{(2\pi/\lambda_0)^2 - k_x^2}$, with λ_0 as the wavelength of the guided wave and k_x as the longitudinal wave vector along the linear array. As k_x takes its maximum at the Brillouin-zone (BZ) boundary $K_B = \pi/a_0$ for a chain of particles, with a_0 being the particle separation, the necessary condition for the system to support the waveguide modes turns out to be [13–15]

$$a_0 < \lambda_0/2. \tag{1}$$

This explains why metallic particles are usually closely spaced in the MPWGs [1–4].

The basic physics, which governs the design of surface-plasmon-based metallic waveguides, applies equally to the dielectric based waveguide. A consequent but interesting issue is whether a SDWG can be developed by arranging dielectric particles into an array under condition (1). If so, the SDWG would not only circumvents the DL but also support nearly lossless EM energy transfer just like conventional dielectric waveguides. Experimentally, the pioneering research was conducted by Quidant and co-workers [16], who used evanescent wave to excite a subwavelength dielectric particle chain and observed the EM energy transfer below the DL. But because, among others [17], condition (1) was not always satisfied in their experiment, and also, the working frequency might not correspond to the frequency of guiding modes; the EM energy attenuates quickly. Theoretically, the SDWGs made of arrays of dielectric particles have been investigated [13–15,18] as well. The theoretical studies suggested that the SDWG should exhibit similar physics as the MPWG: while the waveguide behavior of an array of metallic particles can be understood in the language of the Mie scattering resonances of single particles due to surface plasmons, the same physics can also be expected for dielectric particles with large permittivity. Yet until now no work has been done on manipulating the EM energy transport below the DL with dielectric particle arrays under the photonic circuit conditions, which motivates the current research.

To give an in-principle demonstration, let us first focus on the two-dimensional (2D) case. Consider a chain composed of N parallel infinitely long circular rods with radii $r=100$ nm and separations $a_0=300$ nm. The rods are made of GaAs, whose permittivity has a real part $\varepsilon_c=12.25$ and a negligible imaginary part in the frequency domain $(3.6-34.0)\times 10^{13}$ Hz [14,19]. To examine whether the system can support the energy transfer below the DL, we have to identify the guiding modes. To this end, we employ the rigorous multiple-scattering method [4,20,21], which relates the scattering amplitude $\boldsymbol{a}_{\rm sc}$ from each particle to the amplitude $\boldsymbol{p}_{\rm in}$ of the incoming wave by the $\boldsymbol{T}$ matrix, namely, $\boldsymbol{a}_{\rm sc}=\boldsymbol{T}\boldsymbol{p}_{\rm in}$. We then diagonalize the inverse of the $\boldsymbol{T}$ matrix for different real frequencies. The waveguide modes of the particle chain are characterized by the sharp peaks in $\max\{|[\mathrm{Im}(\lambda_n)]^{-1}|\}$ versus the frequency [22]. Here λ_n is the nth eigenvalue of the matrix $\boldsymbol{T}^{-1}$. For a single particle, a peak in $\max\{|[\mathrm{Im}(\lambda_n)]^{-1}|\}$ corresponds to a Mie resonance [23]. So the waveguide mode of the chain can be understood as a result of collective resonance due to the coupling among the

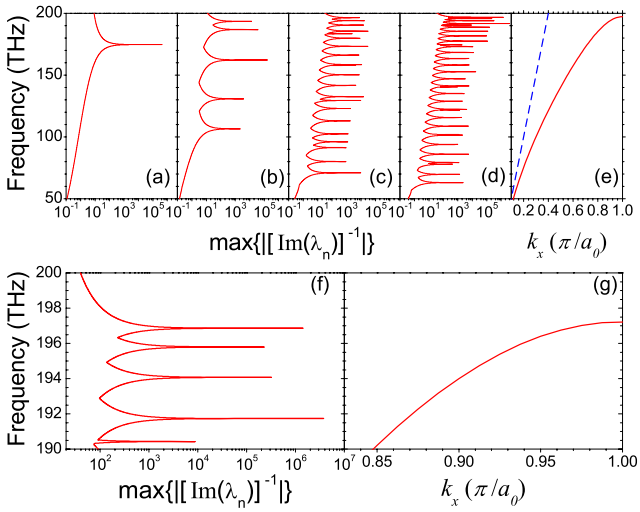

FIG. 1. (Color online) Value of $\max\{|[\mathrm{Im}(\lambda_n)]^{-1}|\}$ versus frequency for (a) a single rod, chains of (b) 5, (c) 20, and (d) 30 rods as well as the photonic band diagram for (e) an infinite array of rods. The light line is shown by the dashed line. Figures (f) and (g) are, respectively, amplified view of (d) and (e) for guiding modes and dispersion band near the BZ boundary.

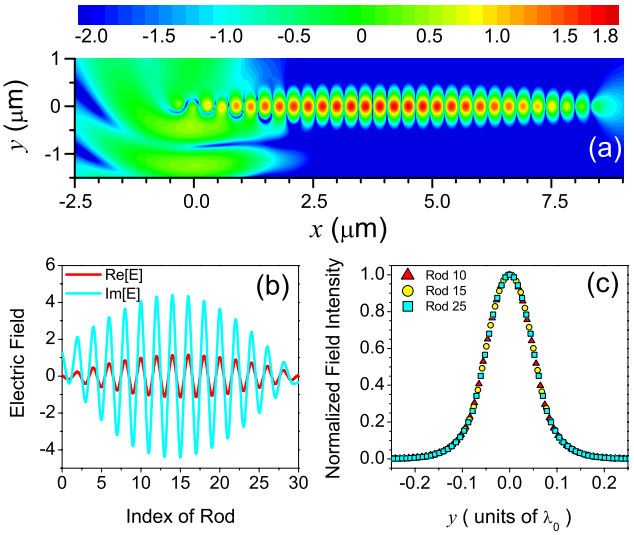

FIG. 2. (Color online) (a) Distribution of the E field intensity (in logarithmic scale) near a chain consisting of 30 rods. The beam, propagating along y, is focused at $x=y=0$, the center of the first rod. (b) The E field at a line parallel to the chain and $1.1r$ above the chain axis. (c) Normalized E field intensity along transverse lines passing different rod centers, with λ_0 the wavelength in vacuum.

Mie resonances of all constituting particles. This is illustrated in Figs. 1(a)–1(e), where the values of $\max\{|[\mathrm{Im}(\lambda_n)]^{-1}|\}$ versus frequency are shown for a single rod as well as for chains of $N=5$, 20, and 30 rods. As N increases, the coupling of the Mie resonances induces an increasing number of guiding modes in chain and, eventually, results in a band below the light line for an infinite array of rods. The mode at higher frequency has k_x closer to the BZ boundary, yielding a better lateral confinement of fields. Our numerical results suggest that the subwavelength lateral confinement can be achieved for all guiding modes with k_x away from the BZ center.

To demonstrate the EM energy transfer below the DL, we illuminate a chain of 30 rods with a transverse magnetic (TM) Gaussian beam that has the electric (E) field polarized along the rod axis and oscillates at frequency $f=19.6874\times10^{13}$ Hz, corresponding to the peak at the highest frequency in Fig. 1(f). The beam has unit E field amplitude at the beam center and waist radius $w_0=\lambda_0$. It is focused on the first rod of the chain. Figure 2(a) shows the 2D pattern of the E field intensity. Though the beam is focused at the center of the first rod, the maximum field intensity appears near rod 15, as can be seen from Fig. 2(b), where the E field on a line parallel to the chain and $1.1r$ above the axis of the chain is shown. The electric field $E_0(j)$ alternates in sign from rod to rod and is well approximated by $\sin[j\pi/(N+1)]\cos(j\pi)$, suggesting a k_x close to the BZ boundary $K_B=\pi/a_0$, where j is the rod index. Figure 2(c) displays the E field intensity along some typical lines transverse to the chain axis. When normalized to the maximum on each line, all data collapse onto a single curve. The E field is confined to the vicinity of the chain, with the full lateral width at half maximum intensity (FLWHM) $w_h<0.12\lambda_0$, indicating the efficient EM energy transfer below the DL along the chain. The results give an explicit demonstration that SDWG could be an alternative for guiding EM energy below the DL, with the advantage of negligible absorption loss.

Integrated optics requires that information be transported around corners [9]. We next turn our attention to the EM energy transfer in a corner structure composed of two linear arrays of N_l rods that make a finite angle θ_l. Typical results are shown in Fig. 3 for $N_l=30$, $\theta_l=60°$, $r=100$ nm, and $a_0=300$ nm. The incident Gaussian beam is centered at the first rod of the horizontal array with $f=19.6854\times10^{13}$ Hz.

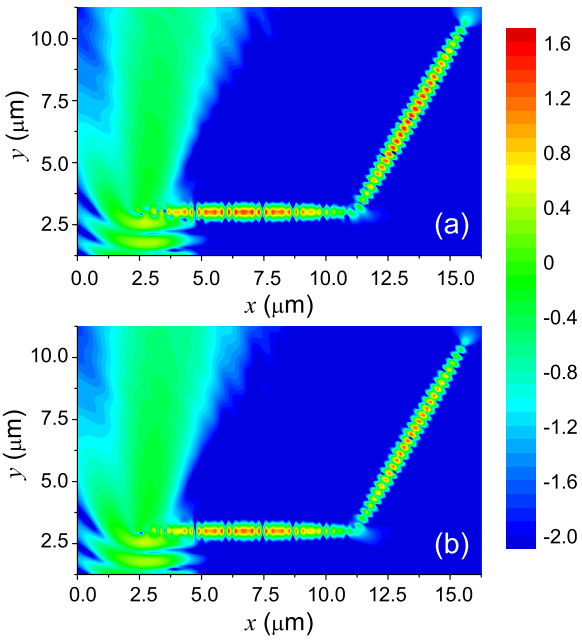

FIG. 3. (Color online) Distribution of E field intensity (in logarithmic scale) near a corner structure (a) without position disorder and (b) with position disorder.

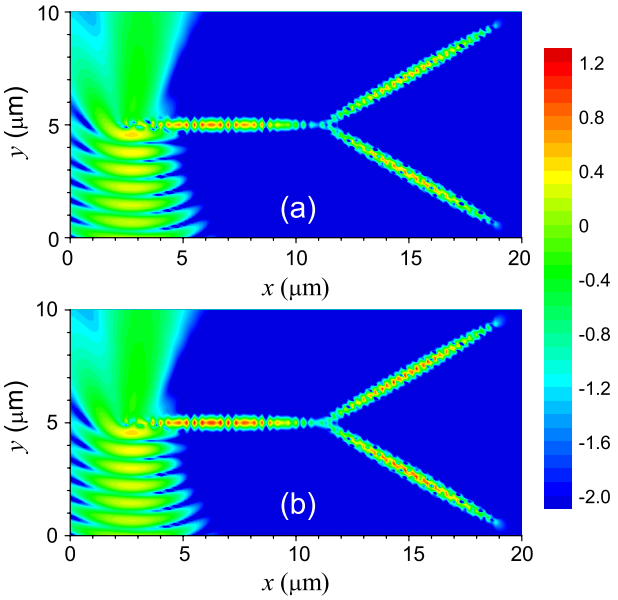

FIG. 4. (Color online) Distribution of the E field intensity (in logarithmic scale) near a bifurcate structure (a) without position disorder and (b) with position disorder.

In Fig. 3(a) we show the E field intensity in the vicinity of the corner structure. It is seen that the EM energy is guided around the corner, with radiative loss nearly suppressed. The field pattern on the side arm is quite similar to that on the horizontal main arm. When $\theta_l \leq 70°$, the maximum E field intensity on the side arm is greater than 90% of that on the main arm [24], implying that the EM energy can make a turn with low loss below the DL.

Another requirement of energy transfer under the photonic circuit conditions is the efficient splitting at a bifurcate structure. To demonstrate this we now focus on energy splitting on a Y-type structure composed of three linear arrays, each consisting of N_y rods, with two forked arrays opening an angle of θ_y. Figure 4 shows a typical case with $N_y=30$ and $\theta_y=60°$. When the horizontal main arm of the Y-shaped structure is illuminated by a TM Gaussian beam with $f=19.6854\times10^{13}$ Hz, the EM energy is seen to transfer along the main arm and split into two parts on two side arms, as shown in Fig. 4(a). The field distributions on two side arms bear close similarity to that on the horizontal main arm illuminated with the beam. Our calculations show that when $\theta_y \leq 80°$, the maximum field intensity on each side arm is larger than 75% of that on the horizontal main arm [24], indicating high efficiency in energy splitting below the DL.

To test the robustness and stability of the SDWG under experimental conditions, we also investigate the effect of the position disorder on energy transport in the corner and bifurcate structures. In our simulations, the rods are allowed to exhibit random displacements normal to the rod axis with a maximum amplitude equal to 5% of the spacing a_0. Typical results are shown in Figs. 3(b) and 4(b), to be compared with Figs. 3(a) and 4(a), respectively. Thirty samples of random position displacements are used here. The average results for 15 samples and 30 samples differ by less than 10%. The field intensity pattern on the side arms still exhibit close resemblance to that on the main arm, suggesting that the energy transfer is not affected obviously. For the corner structure, our calculations show that when $\theta_l \leq 70°$, the maximum field intensity on the side arm is over 80% of that on the main arm. For the bifurcate Y-shaped structure, when $\theta_y \leq 80°$, the maximum field intensity on each side arm remains over 60% of that on the main arm [24].

The MPWG suffers from strong attenuation due to the intrinsic absorption loss. The SDWG is expected to largely circumvent this limitation based on the dielectrics that have negligible loss in some spectral region. Figure 5(a) shows, for a longer chain consisting of 180 GaAs rods, the E field intensity distribution excited by a beam at $f=150$ THz. The rod permittivity is taken as $\varepsilon=12.25+0.02i$, which represents a much bigger loss than the realistic case for GaAs at this frequency regime [19]. The propagation of EM energy is still achieved with extremely small propagation loss [see also Fig. 5(b)]. Figure 5(c) exhibits w_h and v_g versus frequency. It is seen although w_h increases as the frequency decreases (approaches the light line), the energy propagation can still be realized with finite group velocity and subwavelength lateral confinement in a finite frequency regime.

The subwavelength confinement of the EM energy during transport is not limited to the 2D case. A typical 3D example is shown in Fig. 6(a), where the linear array consists of 90 GaAs spheres of radius $r=200$ nm placed at the x axis and separated by $a_0=600$ nm. The incident Gaussian beam of numerical aperture NA=0.9 with $f=19.8525\times10^{13}$ Hz propagates in y direction with the E field polarized along z. The beam is focused at the center of the first sphere in the chain. The propagation of EM energy below the DL over long distance is clearly seen from the distribution of the E field intensity displayed in Fig. 6(a).

Finally, let us make a brief comparison with guiding mo-

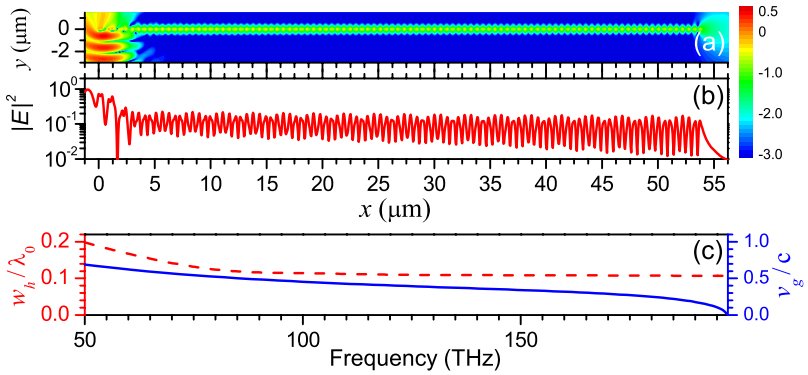

FIG. 5. (Color online) (a) Distribution of the E field intensity (in logarithmic scale) for a chain of 180 rods subject to beam excitation at $f=150$ THz, with rod permittivity taken as $\varepsilon=12.25+0.02i$. (b) The E field intensity at a line parallel to the chain and $1.1r$ above the chain axis, demonstrating small propagation loss. (c) The FLWHM w_h (red dashed line) and the group velocity v_g (blue solid line) versus frequency.

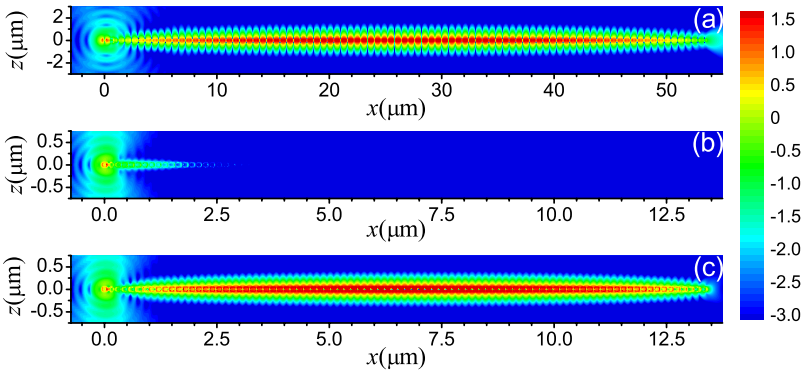

FIG. 6. (Color online) Distribution of the E field intensity (in logarithmic scale) near a chain consisting of 90 spherical particles. The chain is along x and the Gaussian beam, propagating in y with its E field polarized along x, is focused at the center of the first sphere. The 90 particles are made of (a) GaAs with $\varepsilon=12.25$ and (b) Ag with ε given by a modified Drude model (see the text). Figure (c) is obtained by setting $\gamma=0$ in the Drude model, showing the guiding modalities resembling the dielectric particle chain.

dalities of MPWGs. In Fig. 6(b) we show a typical example for MPWGs: a linear chain consisting of 90 Ag spherical particles of $r=50$ nm and $a_0=150$ nm. A modified Drude model of $\varepsilon=\varepsilon_h-(\varepsilon_s-\varepsilon_h)\omega_p^2/(\omega^2-i\gamma\omega)$ is used for Ag, with ω_p, γ, ε_h, and ε_s given in [25]. A Gaussian beam with NA $=0.9$ and wavelength $\lambda_0=370.2$ nm is focused on the center of the first Ag particle. It is seen that, due to the intrinsic absorption loss in Ag, the transport of EM energy suffers from severe attenuation, as shown in Fig. 6(b). The energy attenuation length is around 1 dB/100 nm. If one neglects the material loss by setting $\gamma=0$ in the Drude model, the guiding modalities bear a striking resemblance to that of the SDWG, as can be seen by comparing Fig. 6(c) with Fig. 6(a). This indicates that the energy attenuation in the MPWG is largely due to the intrinsic material loss and can thus be circumvented by the SDWG based on dielectrics of low loss. It is noted that since the Mie resonance is supported even in the point-dipole limit for the metallic case, while a minimum size is required for a dielectric particle to yield a Mie resonance, an MPWG is more competitive in confining wave to an even smaller scale. But the intrinsic loss in the MPWG makes SDWG an alternative for photonic circuit design, with a bit looser (still at a subwavelength level) confinement but much less loss.

In summary, we have demonstrated the manipulation of the EM energy transfer below the DL with the use of dielectric particles, through guiding the EM energy along a straight chain, around a corner, as well as splitting the EM energy at typical bifurcated structures. Our results suggest that dielectric particles with large permittivity can be arranged to localize and guide the EM energy in the subwavelength scale, providing an alternative way toward the integrated optics, with the advantage of negligible intrinsic material loss in comparison with the surface-plasmon-based metallic counterparts.

This work was supported by the China-973 Program, NSFC, MOE of China (Grant No. B06011), PCSIRT, and Shanghai Science and Technology Commission. S.T.C. was partly supported by the (U.S.) DOE.

[1] S. A. Maier, *Plasmonics: Fundamental and Applications* (Springer, New York, 2007).
[2] W. L. Barnes, A. Dereux, and T. W. Ebbesen, Nature (London) **424**, 824 (2003).
[3] S. A. Maier *et al.*, Nature Mater. **2**, 229 (2003).
[4] M. Quinten *et al.*, Opt. Lett. **23**, 1331 (1998).
[5] J. R. Krenn *et al.*, Phys. Rev. Lett. **82**, 2590 (1999).
[6] L. Yin *et al.*, Nano Lett. **5**, 1399 (2005).
[7] R. de Waele, A. F. Koenderink, and A. Polman, Nano Lett. **7**, 2004 (2007).
[8] D. S. Citrin, Nano Lett. **4**, 1561 (2004).
[9] S. A. Maier *et al.*, Adv. Mater. **13**, 1501 (2001).
[10] S. A. Maier, P. G. Kik, and H. A. Atwater, Phys. Rev. B **67**, 205402 (2003).
[11] L. A. Sweatlock, S. A. Maier, H. A. Atwater, J. J. Penninkhof, and A. Polman, Phys. Rev. B **71**, 235408 (2005).
[12] S. A. Maier *et al.*, Appl. Phys. Lett. **86**, 071103 (2005).
[13] A. L. Burin *et al.*, J. Opt. Soc. Am. B **21**, 121 (2004).
[14] G. S. Blaustein *et al.*, Opt. Express **15**, 17380 (2007).
[15] S. T. Chui and Z. Lin, Phys. Rev. E **78**, 065601(R) (2008).
[16] R. Quidant *et al.*, Phys. Rev. E **65**, 036616 (2002).
[17] One of the main reasons is the loss in the third direction of space for the system of heterowires with finite height.
[18] A. Yariv *et al.*, Opt. Lett. **24**, 711 (1999); Ch. Girard, A. Dereux, and C. Joachim, Phys. Rev. E **59**, 6097 (1999); J. C. Weeber *et al.*, *ibid.* **62**, 7381 (2000).
[19] $\mathrm{Im}[\varepsilon]<10^{-4}$ for GaAs in this frequency regime, see, e.g., E. D. Palik, *Handbook of Optical Constants in Solids* (Academic, New York, 1985).
[20] D. Felbacq, G. Tayeb, and D. Maystre, J. Opt. Soc. Am. A Opt. Image Sci. Vis. **11**, 2526 (1994).
[21] E. Centeno and D. Felbacq, J. Opt. Soc. Am. A **16**, 2705 (1999).
[22] A similar method was used in a different context, see, K. H. Fung and C. T. Chan, Opt. Lett. **32**, 973 (2007).
[23] H. C. van der Hulst, *Light Scattering by Small Particles* (Dover, New York, 1981).
[24] The subwavelength waveguides, including MPWGs, serve to localize and guide EM energy in the subwavelength scale rather than acting as weveguides in the conventional sense, see, J. R. Krenn, Nature Mater. **2**, 210 (2003) so the sum of the EM energy on the side arm s may exceed that on the horizontal main arm.
[25] P. G. Kik, S. A. Maier, and H. A. Atwater, Phys. Rev. B **69**, 045418 (2004).